DOI: 10.1002/cbic.200800254

DNA Labeling by Ligand Inducible Secondary Structure

Tao Peng, Hanping He, Masaki Hagihara, and Kazuhiko Nakatani*[a]

Since the human genome sequence has been determined, detection of the nucleotide base at the site of single nucleotide polymorphisms (SNPs) is one of the topics of current chemical research. Simple, accurate, and cost effective methods of SNP typing would be necessary for personalized medicine. Towards this end, a number of SNP typing methods have been investigated and reported.[1,2] Most of these methods required an allele-specific oligonucleotide (ASO) as a probe, which was modified by fluorescent dyes and/or other chemicals as a reporting tag.[3] A drawback of the use of ASO probes was the necessity for the discrimination or separation of a fully matched duplex from a singly mismatched duplex produced by hybridization of ASO probes to the target DNA. In addition, the ASO probes were mostly used after PCR amplification of the DNA samples being tested. The separation of the target strand from the duplex or selective amplification of the target strand by asymmetric PCR was necessary for the effective hybridization of ASO probes. Thus, SNP typing methods that are operational during the amplification process would be more favorable than those postamplification methods from the viewpoint of a simple analytical procedure. On the basis of the accumulated knowledge on SNP typing, the next chemical challenge concerning SNP typing[2] is to propose truly practical methods that are applicable to SNP in any sequence. We report herein, our chemical approach to practical SNP typing based on allele-specific PCR integrated with a new concept of DNA-labeling by ligand-inducible secondary structure (LISS).

PCR is currently one of the most fundamental technologies in biology. Besides the original purpose of amplifying DNA fragments, PCR provides information regarding the presence or absence of a particular DNA sequence in the sample DNA.[3] PCR is recognized as an important tool for reliable diagnosis of infectious diseases and detection of genetic variations.[4,5] Allele-specific PCR (AS-PCR) detects point mutations depending on a match or mismatch base pair between the 3′ terminus of the primer and the template sequence.[6] Allele specificity in PCR would rely on the high fidelity of DNA polymerase in addition to improved primer design.[1a,7] Methods detecting the double stranded DNA produced,[5] pyrophosphate,[8] and a signal and/or fragments produced from reporter DNA probes[9] have been studied for monitoring PCR progress. We have investigated a new concept for labeling PCR primers by LISS to monitor the progress of PCR by detecting the amount of the PCR primer, which would be decreasing as the PCR progresses. The chemical basis of LISS is selective ligand binding to the single stranded DNA, resulting in a large structural change of the DNA. The requirement of structural change on ssDNA reduced the chance of ligand binding to dsDNA, for example, PCR products. The PCR primer was labeled at the 5′-end with a short single stranded tag of the trinucleotide repeat sequence (TRS-tag). We have examined $d(TGG)_n$ as the TRS-tag for labeling the PCR primer, because 1) a single stranded $d(TGG)_n$ sequence does not have stable secondary structures that may interfere with the polymerase reaction, and 2) we have a naphthyridine carbamate dimer (NCD) that binds to the TGG/TGG sequence containing three contiguous T–G, G–G, and G–T mismatches with concomitant flipping out of the thymine (Figure 1).[10] The TGG/TGG sequence is the one of possible sequences when the $d(TGG)_n$ produced a hairpin secondary structure. We anticipated that NCD would bind to the $d(TGG)_n$-tag by inducing a structural change from the single

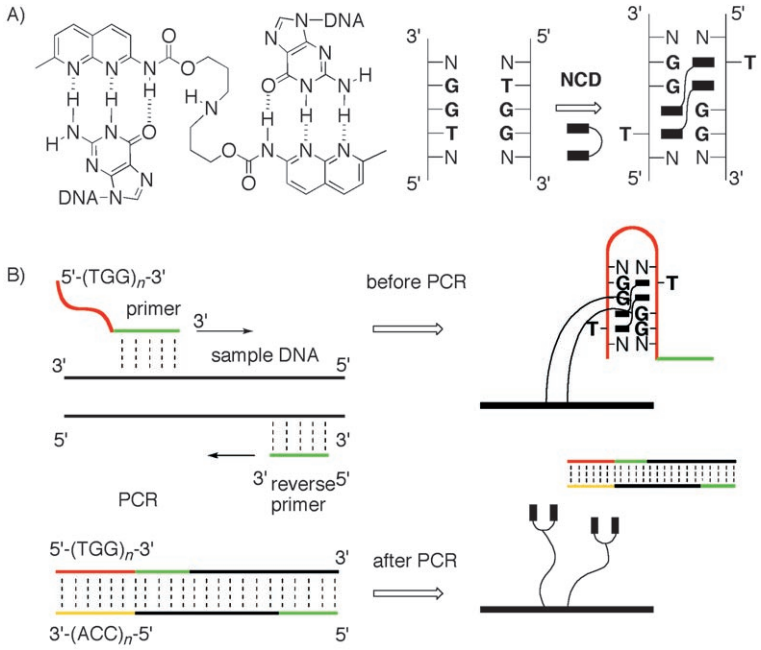

Figure 1. A) Structure of NCD and the mode of NCD binding to the G–G mismatch in the 5′-TGG-3′/5′-TGG-3′ sequence. B) Illustration of PCR with the TRS-tagged primer consisting of a $d(TGG)_n$–tag (red) and a priming sequence (green). The single stranded $d(TGG)_n$-tag in the primer was converted into a double stranded $d(TGG)_n/d(CCA)_n$ by the synthesis of the complementary $d(CCA)_n$ (yellow).

[a] Dr. T. Peng, Dr. H. He, Dr. M. Hagihara, Prof. Dr. K. Nakatani
Department of Regulatory Bioorganic Chemistry
The Institute of Scientific and Industrial Research, Osaka University
8–1 Mihogaoka, Ibaraki, 567–0047 (Japan)
Fax: (+81) 6-6879-8459
E-mail: nakatani@sanken.osaka-u.ac.jp

Supporting information for this article is available on the WWW under http://www.chembiochem.org or from the author.

stranded form to the hairpin secondary structure involving repeats of TGG/TGG in the hairpin stem. As the PCR proceeded, the single stranded $d(TGG)_n$-tag in the primer will be transformed into the duplex $d(TGG)_n/d(CCA)_n$ in the products, which may not be susceptible to the NCD-binding. The relative amount of the $d(TGG)_n$-tagged primer determined with the NCD-immobilized surface plasmon resonance (SPR) sensor before and after PCR would provide information regarding the PCR progress. In fact, PCR progress was successfully monitored by the SPR detection of the $d(TGG)_{10}$-tagged primer with NCD-immobilized sensor. The combination of TRS-tagged primer with allele-specific PCR provided us a practical method of SNP typing, which does not require any ASO probes with chemical-labeling.

We first investigated the NCD binding to the single stranded $d(TGG)_n$ and the double stranded $d(TGG)_n/d(CCA)_n$. The UV-melting profiles of $d(TGG)_4$, $d(TGG)_6$, and $d(TGG)_{10}$ did not show any significant absorption changes (Figure 2A), indicating the absence of particular secondary structures for $d(TGG)_n$. In the presence of NCD, a distinct and sigmoidal increase of the absorption was observed to give the melting temperature at 78 °C for $d(TGG)_4$, 85 °C for $d(TGG)_6$, and 92 °C for $d(TGG)_{10}$. The melting temperature of duplex $d(TGG)_{10}/d(CCA)_{10}$ is 81 °C, which was not affected by NCD (Figure 2B). CD spectra of $d(TGG)_{10}$ showed a large structural change upon binding of NCD with a strong induced CD at the region of the NCD absorption. Appearance of the isodichroic points suggested a smooth structure change from $d(TGG)_{10}$ to NCD-bound $d(TGG)_{10}$. The binding of $d(TGG)_{10}$ to NCD was clearly detected at 100 nM by SPR with the NCD-immobilized sensor (Figure 2D).[11] The short repeat $d(TGG)_6$ needed 1 μM for detection (Figure S1). These binding studies clarified that 1) NCD binds to the single stranded $d(TGG)_n$, but not to the double stranded $d(TGG)_n/d(CCA)_n$ and 2) $d(TGG)_{10}$ will be suitable for the TRS-tag with regard to the sensitivity to the NCD-immobilized SPR sensor.

Having confirmed the selective NCD-binding to single stranded $d(TGG)_n$, we then looked at PCR with the primer having the $d(TGG)_n$-tag and the detection of the $d(TGG)_n$-tagged primer with the NCD-immobilized SPR sensor. PCR was performed with $d(TGG)_6$- and $d(TGG)_{10}$-tagged primers (1 μM) on a template pUC18 and compared to the unlabeled primer. The PCR products were analyzed by PAGE (Figure 3A). The PCR product with a unlabeled primer was 70 bp in length, whereas those with $d(TGG)_6$- and $d(TGG)_{10}$-tagged primers were 88 and 100 bp, respectively. The three PCR products in lanes 2, 4, and 6 showed a different mobility on the gel, indicating that PCR with three primers effectively proceeded and that the $d(TGG)_6$ and $d(TGG)_{10}$-tags attached at the 5′ end of the primer did not interfere with the PCR. The solution of PCR using $d(TGG)_{10}$-tagged primer was analyzed without purification with the NCD-immobilized sensor before and after PCR cycles (Figure 3B). The intensity of the SPR signal at 200 s was 96 response unit (RU) before PCR, whereas the signal decreased to 51 RU after 35 PCR cycles. With unlabeled primer (lacking the $d(TGG)_{10}$-tag), the SPR signal obtained for the PCR solution was about 20 RU under the same analytical conditions, and was virtually unchanged before and after the PCR cycles (Figure S2). Both PAGE and SPR analyses suggested that the decrease in SPR signal by about 45 RU for the PCR solution using the $d(TGG)_{10}$-tagged primer was due to the consumption of the primer.

The potential of PCR using the TRS-tagged primer were investigated with AS-PCR. AS-PCR was investigated for the G at the nucleotide position 375 of pUC18. The nucleotide at the 3′-end of the match primer was C, whereas that of the mismatch primer was A (Figure 3C). These primers were used with the $d(TGG)_{10}$-tag. With the match primer, the change in the SPR intensity for the PCR solution was 41 RU before and after

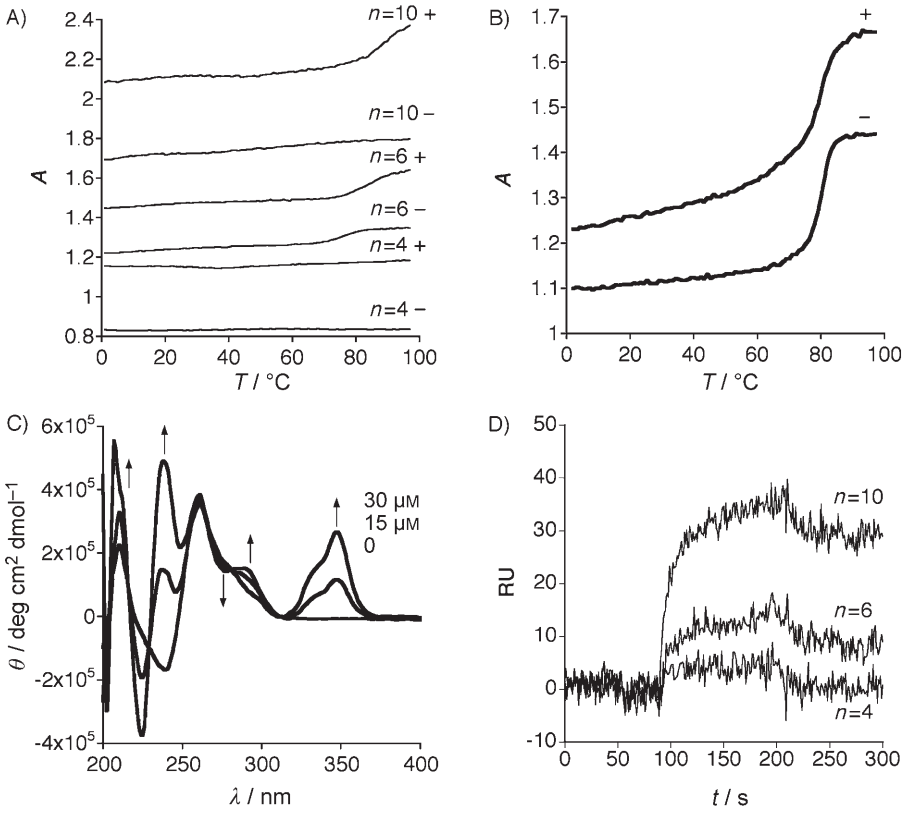

Figure 2. A) The UV-melting profiles of $d(TGG)_n$ (5 μM) ($n=4$, $n=6$, $n=10$) in the absence (–) and presence (+) of NCD (100 μM). B) The UV-melting profile of $d(TGG)_{10}/d(CCA)_{10}$ (2.5 μM) in the absence (–) and presence (+) of NCD (50 μM). C) CD spectra of $d(TGG)_{10}$ (5 μM) in the absence and presence of 15 μM and 30 μM of NCD. D) SPR analyses of 100 nM $d(TGG)_4$, $d(TGG)_6$, and $d(TGG)_{10}$ by the NCD-immobilized sensor.

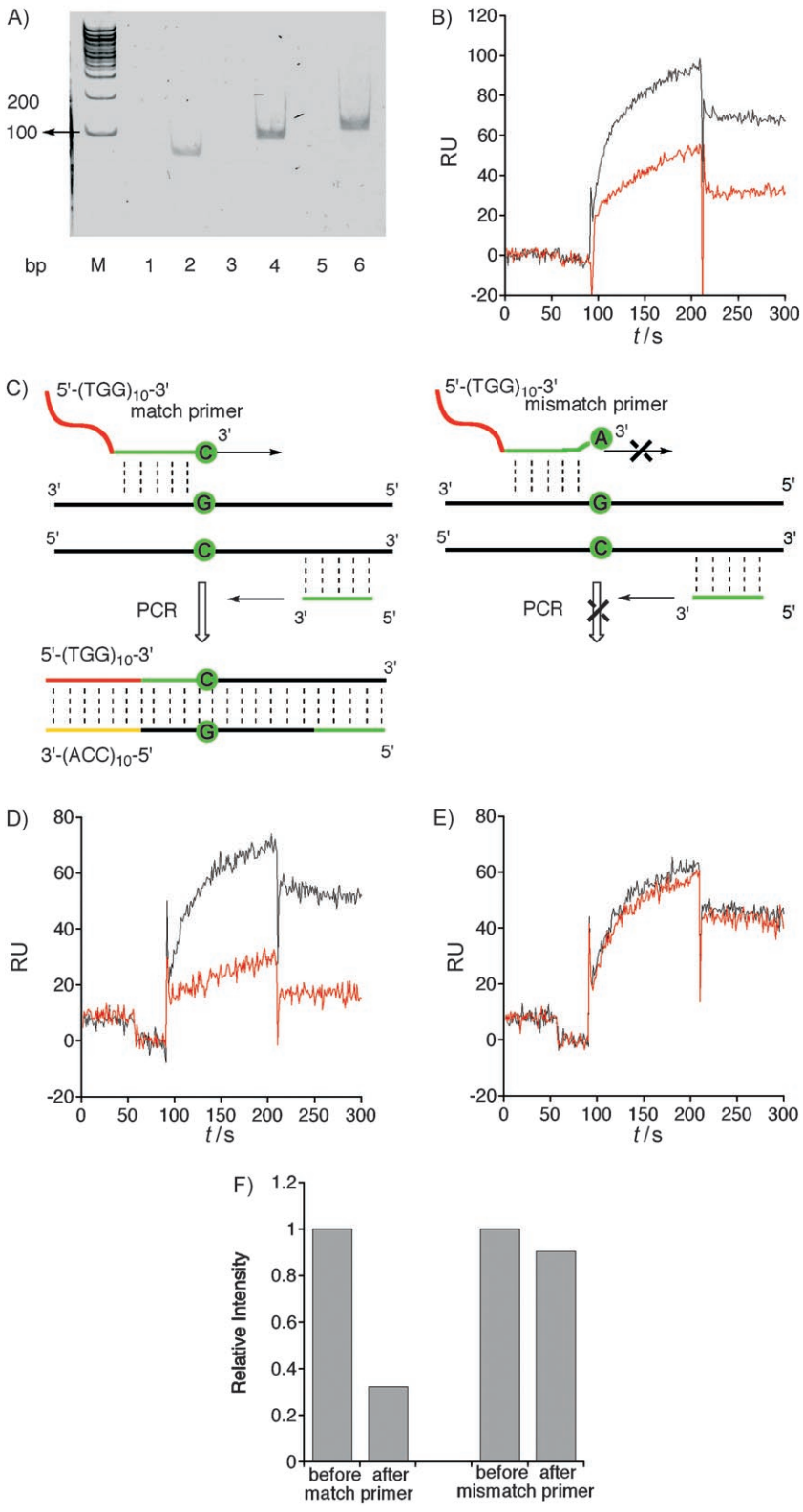

Figure 3. A) The native PAGE analyses of the PCR products. M, 100 bps ladder marker; Lanes 1, 3, and 5, without template; lanes 2, 4, and 6, with pUC18; lanes 1 and 2, unlabeled primer; lanes 3 and 4, $d(TGG)_6$-tagged primer; lanes 5 and 6, $d(TGG)_{10}$-tagged primer. B) SPR analyses of the PCR solution with the $d(TGG)_{10}$-tagged primer before (black) and after PCR (red). C) Illustration of AS-PCR with TRS-tagged primer. D) SPR analyses of the PCR solution with the $d(TGG)_{10}$-tagged match primer. E) SPR analyses of the PCR solution with the $d(TGG)_{10}$-tagged mismatch primer. F) Comparisons of normalized relative intensities of SPR signals before and after PCR corresponding to (D) and (E).

40 PCR cycles (Figure 3D). In marked contrast, only a small decrease (~3 RU) in SPR intensity was observed for the PCR solution with the mismatch primer (Figure 3E). These SPR analyses were in good agreement with those of the PAGE analyses (Figure S3), showing a distinct formation of PCR product with the match primer, but not with the mismatch primer. We have confirmed separately that the progress of PCR was observed for the unlabeled match primer but not for mismatch primer by PAGE analyses (Figure S3).[12]

In the system combining the TRS-tagged primer with the MBL-immobilized SPR detection, the reaction solution after PCR could be measured directly without any treatment by the prepared MBL-immobilized sensor. The detection was performed effectively and finished in less than 10 min, which would be practical and simple for the user. Compared with conventional fluorescent detection with nonsequence specific fluorescent dye, the binding of MBL to the TRS-tag is highly sequence dependent. Another combination of TRS-tag and MBL that is orthogonal to $d(TGG)_n$-tag and NCD in terms of the binding selectivity will be useful for simultaneous SNP typing by multiplex AS-PCR in one tube. Furthermore, the detection of the TRS-tag is not limited to the MBL-immobilized SPR sensor, but can be done by other sensing devices equipped the MBL on its surface. The method depicted herein could provide a simple and rapid way for monitoring PCR, and demonstrate its potential for further advancing current PCR technologies.

Experimental Section

Thermal denaturation profiles: UV melting experiments were carried out with $d(TGG)_n$ (4.5 μM strand) and $d(TGG)_{10}/d(CCA)_{10}$ (2.5 μM) in a 10 mM sodium cacodylate buffer (pH 7.0) and 100 mM NaCl using a SHIMADZU UV-2550 UV-vis spectrometer linked to a Peltier temperature controller. The absorbance of the sample was monitored at 260 nm from 2 to 98 °C with a heating rate of 1 °C min^{-1} in the absence and presence of a ligand (100 or 50 μM).

Circular dichroismic spectral studies: CD experiments were performed on a J-725 CD spectrometer (JASCO). CD spectra of the trinucleotide repeat $d(TGG)_{10}$ (5 μM) were measured at different concentrations of NCD (0, 15, and 300 μM) in 10 mM sodium cacodylate buffer (pH 7.0) and 100 mM NaCl at 25 °C.

PCR: The sequence for PCR: $d(TGG)_{10}$-tagged primer: 5′-TGG TGG TGG TGG TGG TGG TGG TGG TGG TGG GTT TTC CCA GTC ACG A-3′, unlabeled primer: 5′-GTT TTC CCA GTC ACG A-3′, Reverse primer: 5′-TCT AGA GTC GAC CTG C-3′, template: pUC18.

PCR was performed in a total volume of 120 μL containing 2 pg of pUC18, 1 μM of each forward primer, 2 μM reverse primer, 54 μL of milli-Q water, and 60 μL of the Taq DNA polymerase mixture (Qiagen). 50 μL and 70 μL of the reaction mixture was used for the SPR test and PCR, respectively. The amplification was carried out in an automated DNA thermal cycle (Takara PCR Thermal Cycler). The cycling program consisted of one denaturation step of 5 min at 95 °C, followed by 35 cycles of 6 s at 95 °C, 15 s at 55 °C, and 30 s at 75 °C, with final extension 7 min at 75 °C. 20 μL of PCR amplification products were analyzed on 8% polyacrylamide gel for 25 min at 150 V in 0.7×TBE buffer, stained with SYBR Gold nucleic acid gel stain and visualized using Safe Imager (Invitrogen). (Another 50 μL of PCR solution was diluted with 150 μL HBS-N buffer subjected to SPR analysis.)

Allele-specific PCR: The AS-PCR was investigated for the G at the nucleotide position 375 of pUC18. The nucleotide at 3′ end of the match primer was C, and A for the mismatch primer. These primers were used with or without $d(TGG)_{10}$ tag. The sequence for allele-specific PCR: Match unlabeled primer: 5′-GTT TTC CCA GTC ACG AC-3′, mismatch unlabeled primer: 5′-GTT TTC CCA GTC ACG AA-3′, match $d(TGG)_{10}$-tagged primer: 5′-TGG TGG TGG TGG TGG TGG TGG TGG TGG TGG GTT TTC CCA GTC ACG AC-3′, mismatch $d(TGG)_{10}$-tagged primer: 5′-TGG TGG TGG TGG TGG TGG TGG TGG TGG TGG GTT TTC CCA GTC ACG AA-3′, reverse primer: 5′-TCT AGA GTC GAC CTG C-3′, template: pUC18. PCR was performed in a total volume of 120 μL containing 2 pg of pUC18, 1 μM of each forward primer, 1 μM reverse primer, 54 μL of milli-Q water, and 60 μL of Taq DNA polymerase. The amplification was carried out in an automated DNA thermal cycle (Takara PCR Thermal Cycler). The cycling program consisted of one denaturation step of 5 min at 95 °C, followed by 40 cycles of 6 s at 95 °C, 15 s at 55 °C, and 30 s at 75 °C, with final extension 7 min at 75 °C. 20 μL of PCR amplification products were analyzed on 8% polyacrylamide gel for 25 min at 150 V in 0.7×TBE buffer, stained with SYBR Gold nucleic acid gel stain and visualized using Safe Imager (Invitrogen). Another 50 μL of PCR solution was diluted with 150 μL HBS-N buffer and subjected to SPR analysis.

General procedure for SPR binding experiments: All measurements were carried out at 25 °C in a continuous flow of a buffer (10 mM HEPES, pH 7.4) containing NaCl (1 M) at a flow rate 30 μL min^{-1} with a BIAcore 2000 system (BIAcore, Uppsala, Sweden).

Preparation of the NCD-immobilized SPR sensor: NCD was immobilized on a dextran matrix coated gold surface (CM5 chip, BIAcore) through a bivalent linker of N-Boc-aminoaldehyde. First, NCD was tethered by a reductive amination to the linker. Deprotection of Boc-group produced a primary amine, which can be immobilized on the sensor surface by coupling between the amine group and activated carboxyl group on the CM5 chip using the standard method with 1-(3-dimethylaminopropyl)- 3-ethylcarbodiimide hydrochloride (EDCI) and N-hydroxy succinimide (NHS).[8b]

Acknowledgements

This work was supported by a Grant in Aid for Scientific Research (S) (18105006) from the Japan Society for the Promotion of Science (JSPS). HPH is recipient of Postdoctoral Fellowship for Foreign Researchers (06061) from JSPS.

Keywords: allele-specific · ligands · mismatches · PCR · SNP typing

[1] a) M. Strerath, A. Marx, *Angew. Chem.* **2005**, *117*, 8052–8060; *Angew. Chem. Int. Ed.* **2005**, *44*, 7842–7849; b) X. Chen, P. F. Sullivan, *Pharmacogenomics J.* **2003**, *3*, 77–96; c) A. C. Syvänen, *Nat. Rev. Genet.* **2001**, *2*, 930–942; d) P. Y. Kwok, *Annu. Rev. Genomics Hum. Genet.* **2001**, *2*, 235–258; e) N. J. Schork, D. Fallin, J. S. Lanchbury, *Clin. Genet.* **2000**, *58*, 250–264.

[2] a) D. Whitcombe, J. Theaker, S. P. Guy, *Nat. Biotechnol.* **1999**, *17*, 804–807; b) J. Li, G. B. Makrigiorgos, *Nat. Protocols* **2007**, *2*, 50–58; c) P. M. Holland, R. D. Abramson, R. Watson, *Proc. Natl. Acad. Sci. USA* **1991**, *88*, 7276–7280; d) I. A. Nazarenko, B. Lowe, M. Darfler, P. Ikonomi, D. Schuster, A. Rashtchian, *Nucleic Acids Res.* **2002**, *30*, e37.

[3] a) H. A. Erlich, D. Gelfand, J. J. Sninsky, *Science* **1991**, *252*, 1643–1651; b) K. Hayashi, D. E. Yandell, *Hum. Mutat.* **1993**, *2*, 338–346; c) J. B. Ristaino, C. T. Groves, G. R. Parra, *Nature* **2001**, *411*, 695–697.

[4] a) E. Beillard, D. Pallisgaard, V. H. J. Van der Velder, *Luekemia* **2003**, *17*, 2474–2486; b) M. Grompe, *Nat. Genet.* **1993**, *5*, 111–117; c) S. Germer, M. J. Holland, R. Higuchi, *Genome Res.* **2000**, *10*, 258–266; d) A. Haliassos, J. C. Chomel, S. Grandjouan, *Nucleic Acids Res.* **1989**, *17*, 8093–8099.

[5] a) I. M. Mackay, K. E. Arden, A. Nitsche, *Nucleic Acids Res.* **2002**, *30*, 1292–1305; b) N. J. Gibson, *Clin. Chim. Acta* **2006**, *363*, 32–47; c) C. A. Heid, J. Stevens, K. J. Livak, P. M. Williams, *Genome Res.* **1996**, *6*, 986–994.

[6] a) M. V. Myakishev, Y. Khripin, S. Hu, D. H. Hamer, *Genome Res.* **2001**, *11*, 163–169; b) M. Heim, U. A. Meyer, *Lancet* **1990**, *336*, 529–523.

[7] a) R. Kranaster, P. Ketzer, A. Marx, *ChemBioChem* **2008**, *9*, 694–697; b) D. Summerer, N. Z. Rudinger, I. Detmer, A. Marx, *Angew. Chem.* **2005**, *117*, 4791–4794; *Angew. Chem. Int. Ed.* **2005**, *44*, 4712–4715; c) M. Strerath, J. Gaster, D. Summerer, A. Marx, *ChemBioChem* **2004**, *5*, 333–339; d) D. Latorra, K. Campbell, A. Wolter, *Hum. Mutat.* **2003**, *22*, 79–85.

[8] a) M. Margulies, M. Egholm, W. E. Altman, S. Attiya, J. S. Bader, L. A. Bemben, J. Berka, Michael S. Braverman, Y.-J. Chen, Z. Chen, S. B. Dewell, L. Du, J. M. Fierro, X. V. Gomes, B. C. Godwin, W. He, S. Helgesen, C. He Ho, G. P. Irzyk, S. C. Jando, M. L. I. Alenquer, T. P. Jarvie, K. B. Jirage, J.-B. Kim, J. R. Knight, J. R. Lanza, J. H. Leamon, S. M. Lefkowitz, M. Lei, J. Li, K. L. Lohman, H. Lu, V. B. Makhijani, K. E. McDade, M. P. McKenna, E. W. Myers, E. Nickerson, J. R. Nobile, R. Plant, B. P. Puc, M. T. Ronan, G. T. Roth, G. J. Sarkis, J. F. Simons, J. W. Simpson, M. Srinivasan, K. R. Tartaro, A. Tomasz, K. A. Vogt, G. A. Volkmer, S. H. Wang, Y. Wang, M. P. Weiner, P. Yu, R. F. Begley, J. M. Rothberg, *Nature* **2005**, *437*, 376–380; b) M. Ronaghi, *Genome Res.* **2001**, *11*, 3–11; c) M. M. Shi, *Clin. Chem.* **2001**, *47*, 164–172.

[9] a) C. A. Heid, J. Stevens, K. J. Livak, P. M. Williams, *Genome Res.* **1996**, *6*, 986–994; b) A. Giulietti, L. Overbergh, D. Valckx, B. Decallonne, R. Bouillon, C. Mathieu, *Methods* **2001**, *25*, 386–401.

[10] a) T. Peng, C. Dohno, K. Nakatani, *Angew. Chem.* **2006**, *118*, 5751–5754; *Angew. Chem. Int. Ed.* **2006**, *45*, 5623–5626; b) K. Nakatani, S. Hagihara,

Y. Goto, A. Kobori, M. Hagihara, G. Hayashi, M. Kyo, M. Nomura, M. Mishima, C. Kojima, *Nat. Chem. Biol.* **2005**, *1*, 39–43; c) T. Peng, K. Nakatani, *Angew. Chem.* **2005**, *117*, 7446–7449; *Angew. Chem. Int. Ed.* **2005**, *44*, 7280–7283.

[11] For the SPR analyses with sensors having mismatch binding ligands on the surface, see: a) K. Nakatani, S. Sando, I. Saito, *Nat. Biotechnol.* **2001**, *19*, 51–55; b) S. Hagihara, H. Kumasawa, Y. Goto, G. Hayasgi, A. Kobori, I. Saito, K. Nakatani, *Nucleic Acids Res.* **2004**, *32*, 278–286; c) A. Kobori, S. Horie, H. Suda, I. Saito, K. Nakatani, *J. Am. Chem. Soc.* **2004**, *126*, 557–562.

[12] SPR signals with match or mismatch primers almost cannot be observed for unlabeled primer (Figure S4). The signals of PCR solution were about 20 RU before PCR, only 5 RU decrease was observed after PCR.

Received: April 15, 2008
Published online on July 24, 2008

